

# The 2017 Outburst of Swift J1357.2-0933:

## Variable period blue dips with a hot, dense HeII wind

J.A. Paice, P.A. Charles, D. Altamirano, A. Beri, P. Gandhi, M.J. Middleton <sup>a</sup>, James Matthews <sup>b</sup>, D.A.H. Buckley, W. Diaz-Merced, E. Kotze, M.M. Kotze <sup>c</sup>, V.S. Dhillon <sup>d</sup>, T.R. Marsh <sup>e</sup>, J.C.A. Miller-Jones, R.M. Plotkin <sup>f</sup>, R. Misra <sup>g</sup>, D.M. Russell <sup>h</sup>, J. Tomsick <sup>i</sup>

j.a.paice@soton.ac.uk

<sup>a</sup>Dept of Physics & Astronomy, Univ. of Southampton, UK

<sup>b</sup>Astrophysics, Univ. of Oxford, UK

<sup>c</sup>South African Astronomical Observatory, Cape Town, South Africa

<sup>d</sup>Dept of Physics & Astronomy, Univ. of Sheffield, UK

<sup>e</sup>Dept of Physics, Univ. of Warwick, UK

<sup>f</sup>ICRAR, Curtin University, Perth, Australia

<sup>g</sup>ICAA, Pune, India

<sup>h</sup>New York University, Abu Dhabi, UAE

<sup>i</sup>Space Sciences Lab., Univ. of California, Berkeley, USA

### Abstract

Quasi-simultaneous optical (ULTRACAM/NTT, SALT), X-ray (NuSTAR, XRT/Swift) and radio(ATCA) observations of the short  $P$ , high latitude LMXB transient, Swift J1357.2-0933 during its 2017 outburst have revealed remarkable additional properties. In addition to confirming the variable frequency optical dipping seen during its 2011 discovery outburst, we also find: (1) the dip shape is consistent with partial disc occultations, (2) the source becomes significantly bluer during these dips, indicating an unusual geometry compared to other LMXB dippers, (3) there is no X-ray response to the optical dips, (4) HeII and Balmer absorption is present only during the dips, and is blue-shifted by  $\sim 600 \text{ km s}^{-1}$ . These spectral features imply a very hot ( $T_e \sim 40,000\text{K}$ ), dense ( $n \sim 10^{13-14} \text{ cm}^{-3}$ ) outflowing wind driven by a central  $L_X \geq 10^{36} \text{ erg s}^{-1}$ . Its periodic visibility implies a very high viewing inclination, and a warped inner disc structure that moves out during the outburst. This is also consistent with its low observed  $F_X/F_{\text{opt}}$  ratio, implying that it is an Accretion Disc Corona (ADC) source, and *not* a VFXT (very faint X-ray transient).

This poster represents a summary of results presented in Paice et al 2019 (MNRAS 488, 512; P19) and Charles et al 2019 (MNRAS in press; Ch19) - all figures are taken from these papers.

## Introduction to Swift J1357.2-0933

- XRT discovered by Swift BAT in 2011
- high latitude ( $b \sim +50^\circ$ )
- initially thought  $d \sim 1.5\text{kpc} \rightarrow \text{VFXT}$  with  $L_X \sim 10^{35} \text{ erg s}^{-1}$ , ruled out by lack of donor features in quiescence
- key feature: Corral-Santana et al. 2013 (A&A 587, A61; CS13) discovered fast ( $\sim$ minutes) optical dipping whose period changed as the outburst progressed!
- dips interpreted by CS13 as structure in inner disc (“torus”) that moved out as outburst progressed ( $P_{\text{dip}} = \text{Keplerian } P$  at that radius), hence high inclination
- CS13 found  $P_{\text{orb}} = 2.8\text{h}$  from H $\alpha$  outburst spectroscopy, consistent with BH object ( $\sim 9M_\odot$ ) and very low mass donor

## 2017 X-ray and Optical Variability

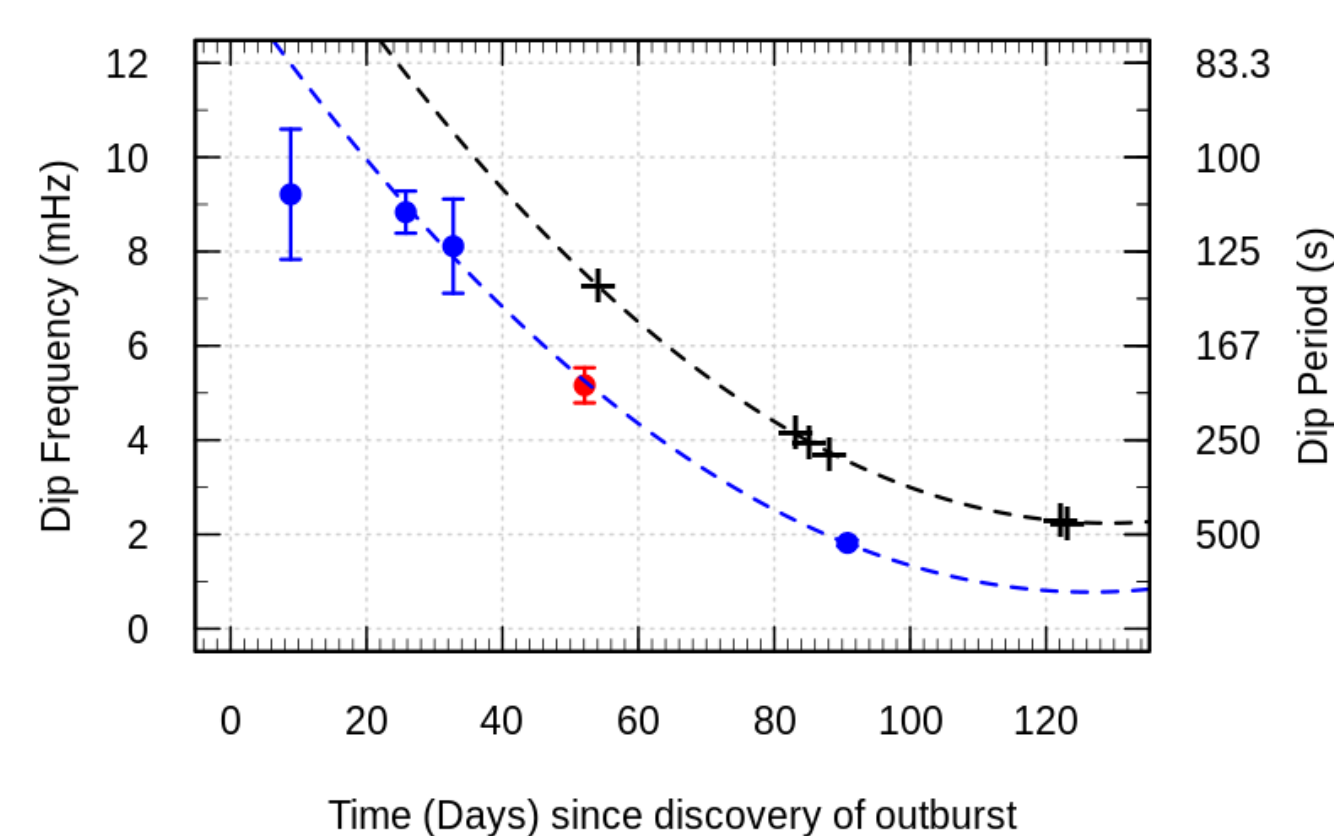


**Figure 1:** Dip frequency evolution of the 2011 (black) and 2017 (blue, red; SALT, ULTRACAM/NTT) outbursts. Fits are parabolic (see CS13, P19).

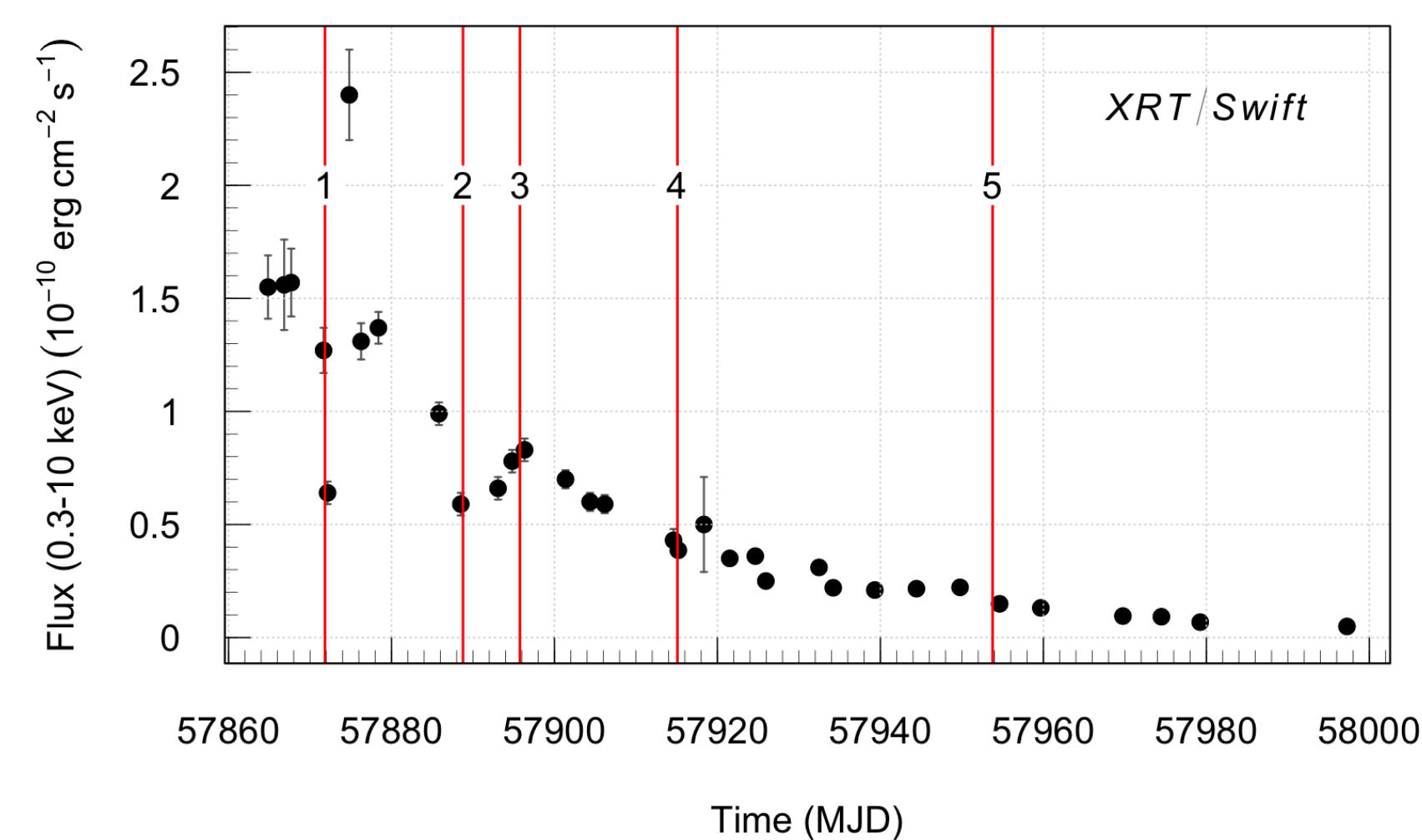


**Figure 2:** Timeline of Swift J1357.2-0933 2017 outburst with red lines marking key observation dates (1-SALT+NuSTAR; 2-SALT+Swift+ATCA; 4-ULTRACAM+NuSTAR+Swift). From P19.

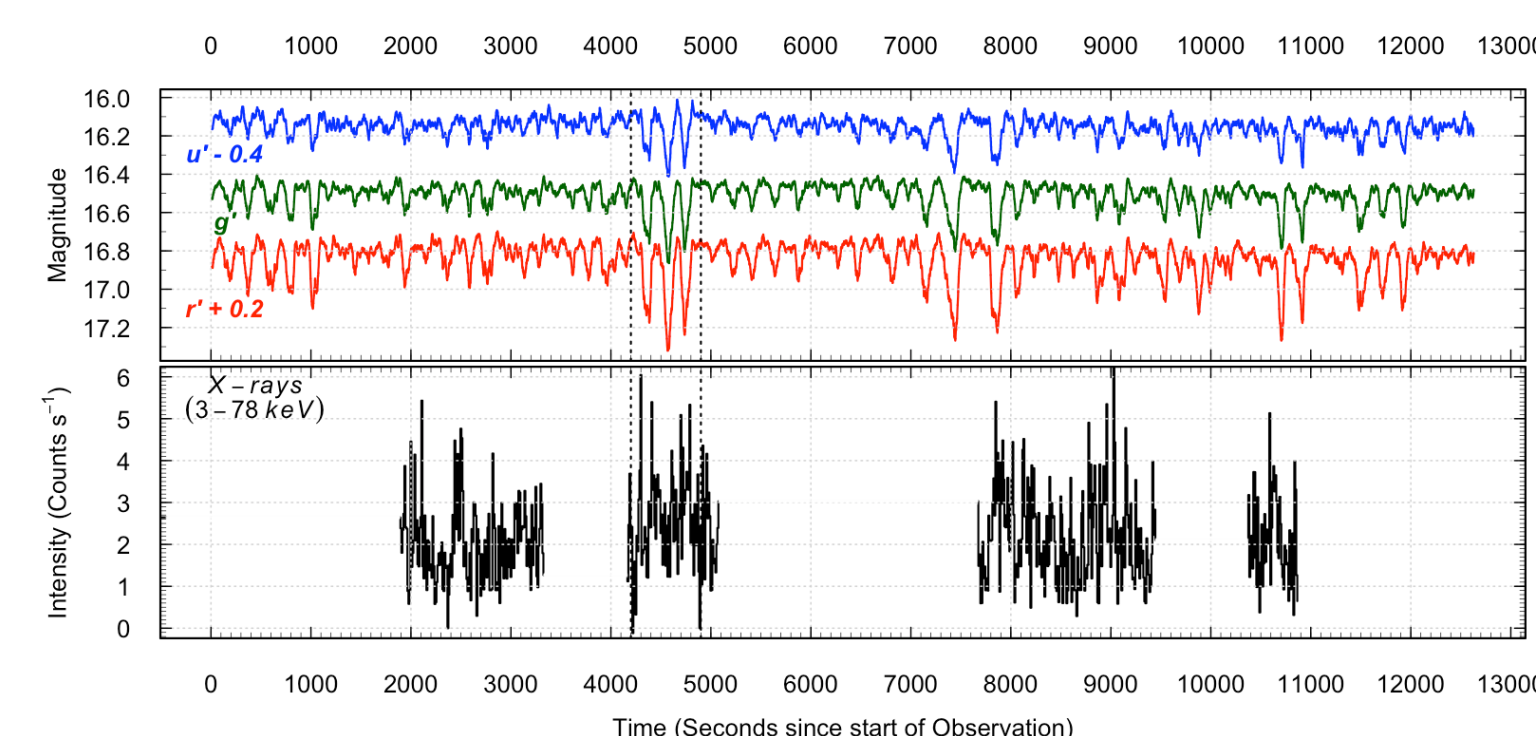


**Figure 3:** ULTRACAM (top) and NuSTAR (bottom) simultaneous lightcurves from 2017 Jun 10/11. Optical data has been binned with a moving average function to better show the long term trends. Note the numerous dips that occur throughout the lightcurve in optical, and the lack of any distinct dips in the X-rays. From P19.

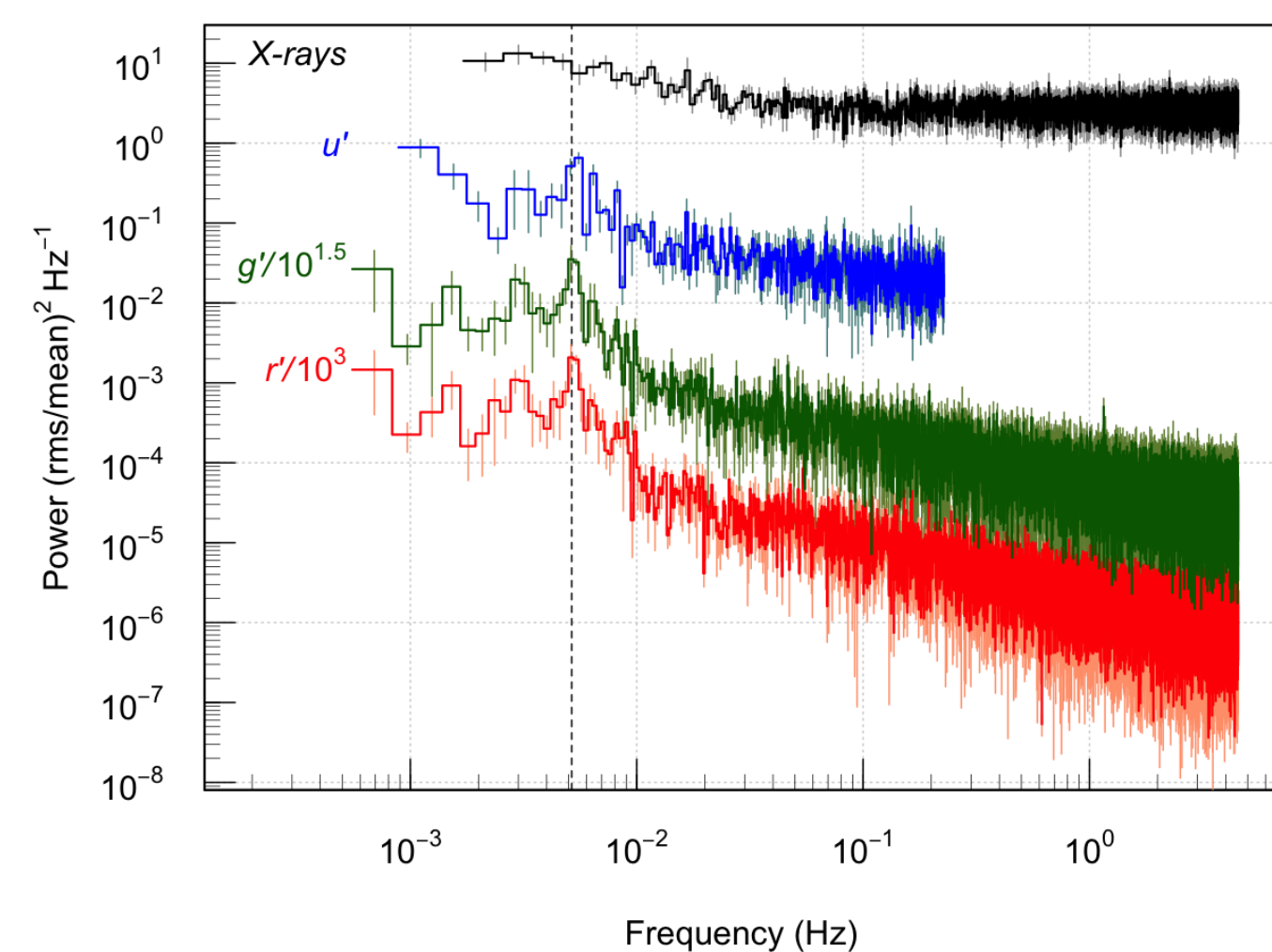


**Figure 4:** X-ray (NuSTAR) and optical (ULTRACAM  $u'$ ,  $g'$ ,  $r'$ ) PSDs of J1357. Note the optical peak at  $\sim 5 \text{ mHz}$  (the dip frequency) and the absence of any X-ray peak. From P19.

## Blue dips

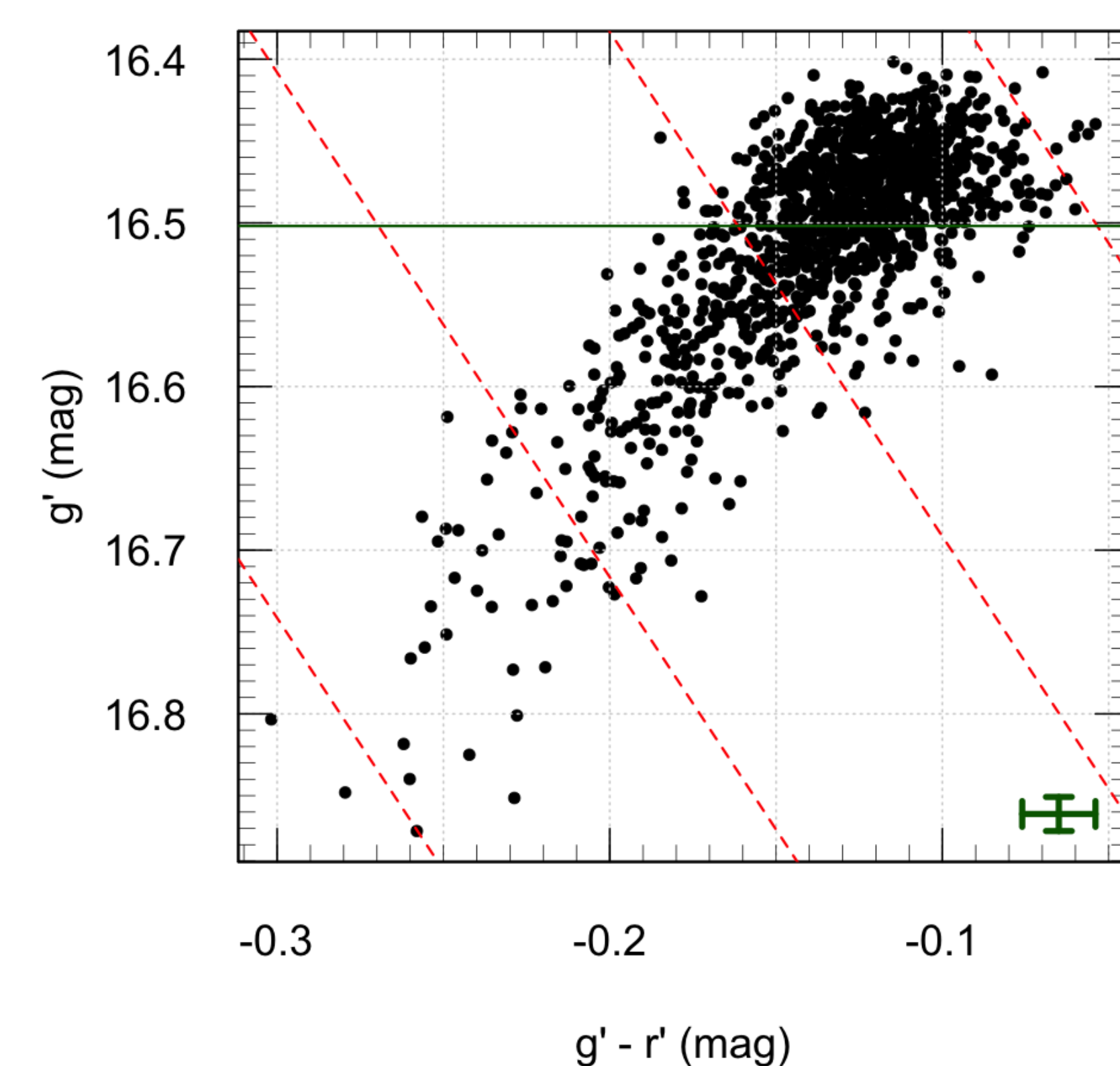


**Figure 5:** ULTRACAM colour-magnitude diagram which shows how blue the (fainter) dip points are, moving orthogonally to that expected for dust obscuration (red dashed lines). The solid green line is the  $g'$  median level. From P19.



## Conclusions

- J1357 has 2 unique properties (variable  $P$  dipping, HeII absorption) amongst all LMXBs
- dips are blue, requiring multiple emitting components of differing colours, e.g. recessed disc or jet
- the strong, absorption-line-only, hot, dense wind implies a very high orbital inclination
- wind requires high  $L_X$ , hence it must be an ADC and at a distance  $\geq 6 \text{ kpc}$

## SALT time-resolved spectra reveal hot, dense, outflowing wind

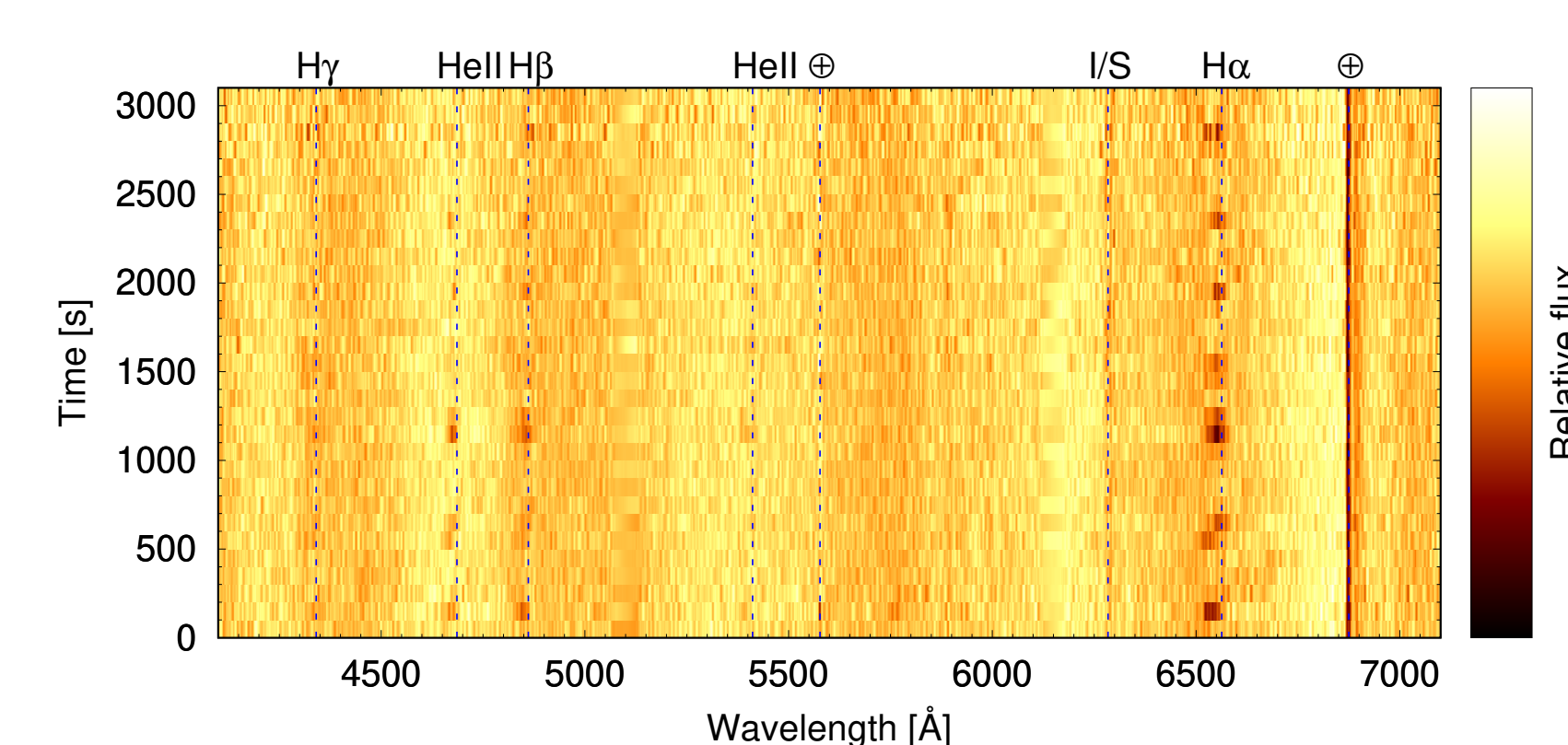


**Figure 6:** SALT time-series spectra of J1357 on 2017 Jul 21, when the dip period was  $\sim 500\text{s}$ . Note the strong HeII  $\lambda 4686$  and H $\beta$  variations associated with the dip frequency. From Ch19.

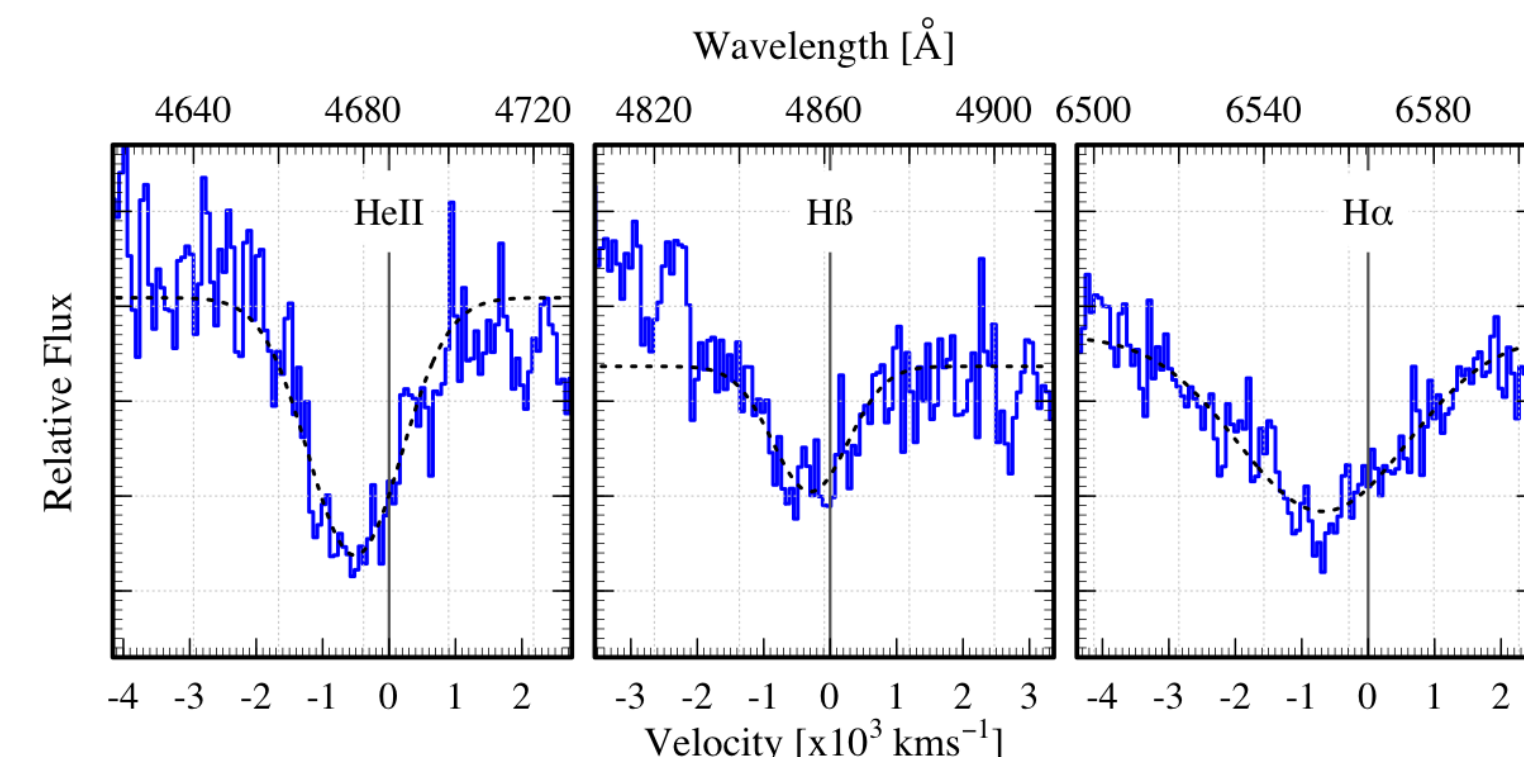


**Figure 7:** HeII, H $\beta$  and H $\alpha$  profiles from mean of four SALT RSS spectra of J1357.2 when these features were strongest on 2017 Jul 21. Gaussian fits are shown, and velocities are relative to rest wavelength, demonstrating the  $\sim 600 \text{ km s}^{-1}$  outflow. From Ch19.

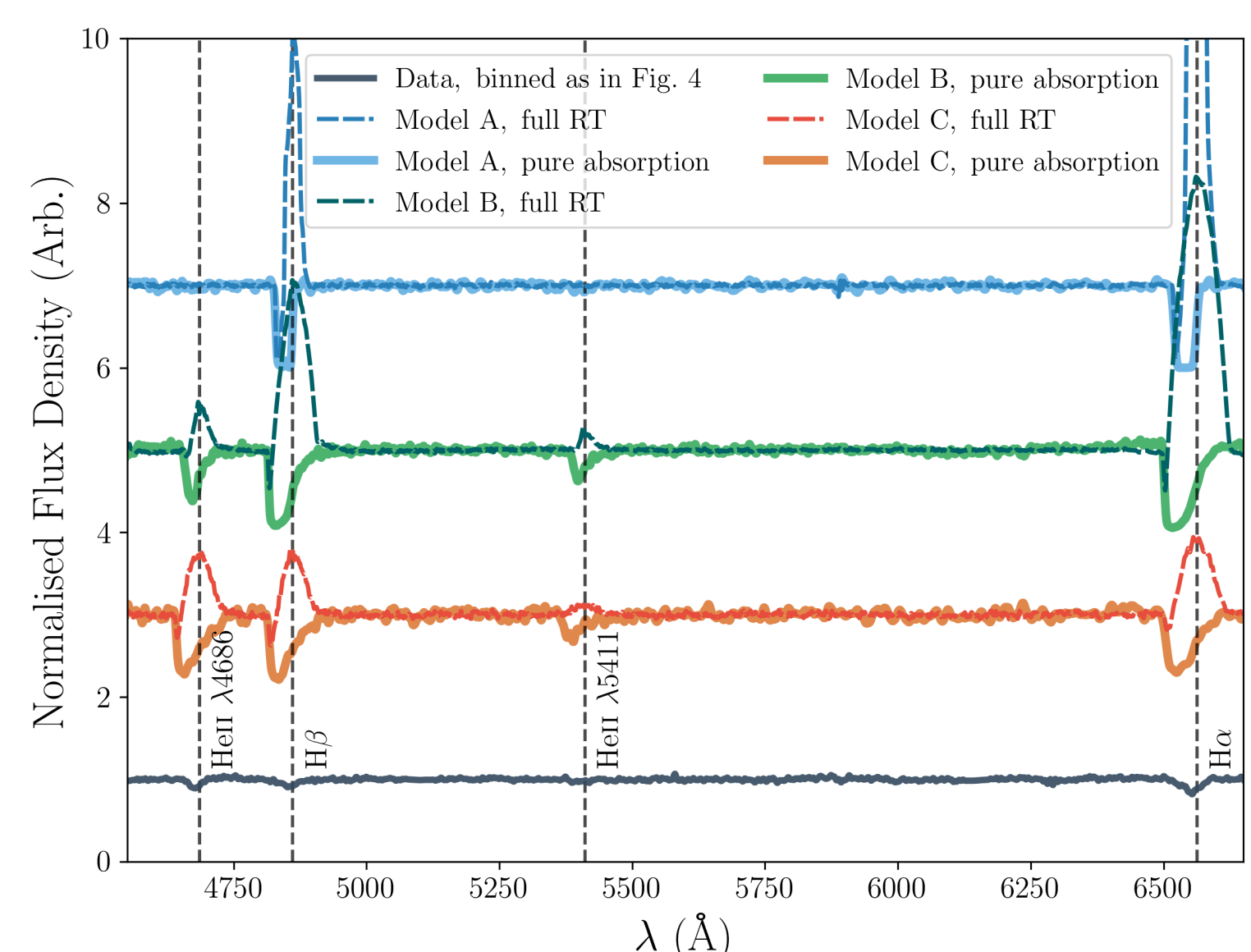


**Figure 8:** Continuum normalised model spectra, calculated with full radiative transfer and in the pure absorption limit, compared to (bottom) RSS spectrum. We show three models that produced obvious and/or Balmer absorption lines: Model A ( $\dot{M}_{w,\text{iso}} = 10^{-7} M_\odot \text{ yr}^{-1}$ ,  $L_{2-10} = 10^{35} \text{ erg s}^{-1}$ ,  $\beta = 4$ ), Model B ( $\dot{M}_{w,\text{iso}} = 10^{-6} M_\odot \text{ yr}^{-1}$ ,  $L_{2-10} = 10^{36} \text{ erg s}^{-1}$ ,  $\beta = 0.5$ ), and Model C ( $\dot{M}_{w,\text{iso}} = 10^{-5} M_\odot \text{ yr}^{-1}$ ,  $L_{2-10} = 10^{37} \text{ erg s}^{-1}$ ,  $\beta = 0.5$ ). From Ch19.

### Acknowledgements

See P19 and Ch19 for full details of the extensive observatory facilities utilised in these studies.